AIMS Mathematics, 7(6): 10234–10244.
DOI: 10.3934/math.2022569
Received: 20 January 2022
Revised: 12 March 2022
Accepted: 16 March 2022
Published: 22 March 2022

http://www.aimspress.com/journal/Math

Research article

Numerical simulation of the space fractional (3 + 1)-dimensional Gray-Scott models with the Riesz fractional derivative

Dan-Dan Dai[1], **Wei Zhang**[2,*] **and Yu-Lan Wang**[3,*]

[1] School of Physics and Electronic Information Engineering, Jining Normal University, Jining 012000, Inner Mongolia, China

[2] Institute of Economics and Management, Jining Normal University, Jining 012000, Inner Mongolia, China

[3] Department of Mathematics, Inner Mongolia University of Technology, Hohhot, 010051, China

* **Correspondence:** Email: jnsfxyzw@163.com, wylnei@163.com; Tel: +864716575470; Fax: +864716575863.

Abstract: The reaction-diffusion process always behaves extremely magically, and any a differential model cannot reveal all of its mechanism. Here we show the patterns behavior can be described well by the fractional reaction-diffusion model (FRDM), which has unique properties that the integer model does not have. Numerical simulation is carried out to elucidate the attractive properties of the fractional (3+1)-dimensional Gray-Scott model, which is to model a chemical reaction with oscillation. The Fourier transform for spatial discretization and fourth-order Runge-Kutta method for time discretization are employed to illustrate the fractal reaction-diffusion process.

Keywords: numerical simulation; patterns; Fourier spectral method; Riesz fractional derivative
Mathematics Subject Classification: 65M30, 65D20

1. Introduction

Reaction-diffusion equations have been widely used to describe various scientific phenomena in mathematics, physics and chemistry. Patterns are non-uniform macrostructure with some regularity in time or space, which can describe the pattern formation by a reaction-diffusion model [1–3]. Pattern exists in nature universally. The stable state will be unstable under certain conditions and spontaneously produce the spatial stationary pattern, namely Turing pattern. From the thermodynamic view, patterns can be divided into two types. The first type of pattern exists in thermodynamic equilibrium conditions, such as crystal structure in inorganic chemistry, organic polymer self-organizing pattern; the second category of patter is the pattern generated under the condition of leaving the thermodynamic

equilibrium state, such as the strip cloud in the sky, the wave on the water surface, the pattern on the body surface of animals, etc. The second type of pattern generate under the condition of thermodynamic equilibrium, such as the strip cloud in the sky, the wave on the water surface, the pattern on the body surface of animals, etc. For the first type of spot pattern, people have a systematic and in-depth understanding. Fractional calculus was recently introduced in many fields, including applied mathematics, electrochemistry, image processing, viscoelasticity, control theory, biology, and neurodynamics. In the last three decades, the theory of fractional calculus [4–9] has successfully been applied to the study of anomalous diffusion motion, because fractional differential equations [10–14] can better model discontinous problems than the traditional differential ones.

The fractional reaction diffusion system can describe anomalous diffusion motion. In this paper, we solve the fractional-in-space 3D coupled Gray-Scott models is as

$$\begin{cases} \dfrac{\partial u}{\partial t} = -K_u(-\Delta^{\frac{\alpha}{2}})u - uv^2 + F(1-u), \\ \dfrac{\partial v}{\partial t} = -K_v(-\Delta^{\frac{\beta}{2}})v + uv^2 - (F+k)v, \end{cases} \tag{1.1}$$

with the initial conditions

$$u(x,y,z,0) = u_0(x,y,z), \quad v(x,y,z,0) = v_0(x,y,z). \tag{1.2}$$

where $(x,y,z,t) \in \Omega \times [0,T]$, $\Omega = (a,b) \times (a,b) \times (a,b)$ and $1 < \alpha,\beta \leq 2$. F and k are arbitrary constants. K_u, K_v are the diffusion coefficients. Fractional Laplacian operator defined by Riesz fractional derivative has the following form

$$\Delta^{\frac{\alpha}{2}}u = D_x^\alpha u + D_y^\alpha u + D_z^\alpha u. \tag{1.3}$$

Definition 1.1. *The Riesz potential and the conjugate Riesz potential [15, 16] of the order $\alpha \in (0,1)$ are the following integrals:*

$$R_x^\alpha u(x) = \frac{1}{2\Gamma(\alpha)\cos\frac{\pi\alpha}{2}} \int_{-\infty}^{\infty} \frac{1}{|x-\tau|^{1-\alpha}} u(\tau)d\tau, \quad x \in R. \tag{1.4}$$

$$H_x^\alpha u(x) = \frac{1}{2\Gamma(\alpha)\sin\frac{\pi\alpha}{2}} \int_{-\infty}^{\infty} \frac{sgn(x-\tau)}{|x-\tau|^{1-\alpha}} u(\tau)d\tau, \quad x \in R. \tag{1.5}$$

If $\alpha > 0, \beta > 0$ and $\alpha + \beta < 1$, then Riesz potential and the conjugate Riesz potential have the following proposition.

$$R_x^\alpha R_x^\beta u(x) = R_x^{\alpha+\beta}u(x), \quad H_x^\alpha H_x^\beta u(x) = H_x^{\alpha+\beta}u(x), \quad x \in R \tag{1.6}$$

Definition 1.2. *The Riesz fractional derivative [17–19] of order $\alpha \in (0,1)$ is given by*

$$D^\alpha u(x) = \frac{d}{dx}H_x^{1-\alpha}u(x) = \frac{1}{2\Gamma(1-\alpha)\cos\frac{\pi\alpha}{2}} \frac{d}{dx} \int_{-\infty}^{\infty} \frac{sgn(x-\tau)}{|x-\tau|^\alpha} u(\tau)d\tau, \quad x \in R. \tag{1.7}$$

The Fourier transforms of $R^\alpha g$ and Riesz fractional derivative for $\alpha \in (0,1)$ are presented as

$$\mathcal{F}[R_x^\alpha u(x)](\omega) = \frac{1}{|\omega|^\alpha}\hat{u}(\omega), \quad \mathcal{F}_x[D_x^\alpha u(x)](\omega) = |\omega|^\alpha \hat{u}(\omega) \tag{1.8}$$

where the Fourier transform and inverse Fourier transform of function $u(x)$ about x definition as:

$$\begin{aligned} \hat{u}(\omega) &= \mathcal{F}_x[u(x)](\omega) = \int_{-\infty}^{\infty} u(x)e^{-i\omega x}\,dx, \\ u(x) &= \mathcal{F}_x^{-1}[\hat{u}(\omega)](x) = \frac{1}{2\pi}\int_{-\infty}^{\infty} \hat{u}(\omega)e^{i\omega x}\,d\omega. \end{aligned} \tag{1.9}$$

A representative bistable system is the coupled Gray-Scott model, and this model is a variant of the autocatalytic Selkov model of glycolysis and is due to Gray and Scott [20, 21]. In [22], authors used time finite element method to solve the two dimensional space fractional Gray-Scott model. In [23, 24], authors used the Fourier spectral method to solve a class of fractional reaction-diffusion equations. In [25], authors used weighted shifted Grünwald difference operator for spatial discretization and the Crank-Nicolson scheme for time discretization to solve the space fractional Gray-Scott model, and so on [26–29].

Numerical methods for solving nonlinear space fractional reaction-diffusion equation have finite difference predictor-corrector method [30, 31], finite difference method [32], reproducing kernel method [33–40], matrix approach method [41], spectral method [42–44], and so on [45, 46]. Accurate and time-saving numerical methods are needed for the study of fractional order dynamical systems and their related phenomena, such as patterns and chaos.

In this manuscript, we use Fourier spectral method for spatial discretization and the Runge-Kutta method for time discretization to solve the space fractional 3D coupled Gray-Scott models with the Riesz fractional derivative. It is found that the results of numerical experiments are consistent with those of other scholars, which verifies the accuracy of the method. We observe some new numerical solutions of space fractional 3D coupled Gray-Scott models which are unlike any that have been previously obtained in numerical or theoretical studies. The present theory can be extened to the fractal-fractional differential equations.

This paper is organized as follows. In Section 2, we introduce numerical method. Numerical experiments are provided in Section 3. Section 4 is conclusion.

2. Numerical method

In order to normalize the space interval $[a, b]$ to $[0, 2\pi]$, we let $x \to \frac{2\pi(x-a)}{L}, y \to \frac{2\pi(y-a)}{L}, z \to \frac{2\pi(z-a)}{L}$ and $L = b - a$, $x_k = k\Delta x = \frac{2\pi Lk}{N}$, $y_k = k\Delta y = \frac{2\pi Lk}{N}$, $z_k = k\Delta z = \frac{2\pi Lk}{N}$, $N > 0$ and N is an integer, $k = 0, 1, \cdots\cdots, N-1$.

Using the following discrete Fourier transform (2.1) for u, v in spatial domain.

$$\begin{aligned} \hat{u}(l_x, l_y, l_z, t) &= \mathcal{F}(u) = \frac{1}{N^3}\sum_{i=0}^{N-1}\sum_{i=0}^{N-1}\sum_{i=0}^{N-1} u(x_i, y_i, z_i, t)e^{-il_x x_i - il_y y_i - il_z z_i}, \\ \hat{v}(l_x, l_y, l_z, t) &= \mathcal{F}(v) = \frac{1}{N^3}\sum_{i=0}^{N-1}\sum_{i=0}^{N-1}\sum_{i=0}^{N-1} v(x_i, y_i, z_i, t)e^{-il_x x_i - il_y y_i - il_z z_i}, \end{aligned} \tag{2.1}$$

where $-\frac{N}{2} \le l_x, l_y, l_z \le \frac{N}{2} - 1$. Equation (1.1) can be transformed into the following ordinary differential equations about t.

$$\begin{cases} \dfrac{\partial \hat{u}}{\partial t} = -K_u(|l_x|^\alpha + |l_y|^\alpha + |l_z|^\alpha)\hat{u} + \mathcal{F}(-uv^2 + F(1-u)), \\ \dfrac{\partial \hat{v}}{\partial t} = -K_v(|l_x|^\beta + |l_y|^\beta + |l_z|^\beta)\hat{v} + \mathcal{F}(uv^2 - (F+k)v), \\ \hat{u}(x,y,z,0) = \hat{u}_0(x,y,z), \quad \hat{v}(x,y,z,0) = \hat{v}_0(x,y,z). \end{cases} \tag{2.2}$$

The fourth-order Runge-Kutta method is used to solve the ordinary differential equation (2.2). Then, we use the following inverse discrete Fourier transform (2.3), and can obtain the numerical solution.

$$\begin{aligned} u(x_i, y_i, z_i, t) &= \mathcal{F}^{-1}(\hat{u}) = \sum_{l_x=-\frac{N}{2}}^{\frac{N}{2}-1} \sum_{l_y=-\frac{N}{2}}^{\frac{N}{2}-1} \sum_{l_z=-\frac{N}{2}}^{\frac{N}{2}-1} \hat{u}(l_x, l_y, l_z, t) e^{il_x x_i + il_y y_i + il_z z_i}, \\ v(x_i, y_i, z_i, t) &= \mathcal{F}^{-1}(\hat{v}) = \sum_{l_x=-\frac{N}{2}}^{\frac{N}{2}-1} \sum_{l_y=-\frac{N}{2}}^{\frac{N}{2}-1} \sum_{l_z=-\frac{N}{2}}^{\frac{N}{2}-1} \hat{v}(l_x, l_y, l_z, t) e^{il_x x_i + il_y y_i + il_z z_i}, \end{aligned} \tag{2.3}$$

where $0 \le i \le N-1$. If $\alpha = \beta$, Eq (2.2) can be reduced the following form:

$$\begin{cases} \frac{\partial W}{\partial t} = R(t, W), \\ W(K\alpha, 0) = W_0. \end{cases} \tag{2.4}$$

where

$$\begin{aligned} &\hat{\phi} = \begin{pmatrix} \hat{u} \\ \hat{v} \end{pmatrix}, \quad r(t, \hat{\phi}) = \begin{pmatrix} \frac{\partial \hat{u}}{\partial t} \\ \frac{\partial \hat{v}}{\partial t} \end{pmatrix}, \quad K\alpha = -(|l_x|^\alpha + |l_y|^\alpha + |l_z|^\alpha), \\ &W = (\hat{\phi}_0(K\alpha, t), \hat{\phi}_1(K\alpha, t), \cdots, \hat{\phi}_{N-1}(K\alpha, t))^T, \\ &R(t, W) = (r_0(t, \hat{\phi}_0(t)), r_1(t, \hat{\phi}_0(t)), \cdots, r_{N-1}(t, \hat{\phi}_{N-1}(t)))^T, \\ &W_0(K\alpha) = (\hat{\phi}_{00}(K\alpha), \hat{\phi}_{01}(K\alpha), \cdots, \hat{\phi}_{0(N-1)}(K\alpha))^T, \end{aligned} \tag{2.5}$$

τ is step-size and $n = 1, \cdots, \frac{T}{\tau}$.

Definition 2.1. A class of single-step method for solving ordinary differential equation in the form of:

$$W_{n+1} = W_n + \tau\psi(W_n, t_n, \tau), \tag{2.6}$$

where incremental function $\psi(W_n, t_n, \tau)$ is determined by $R(t, U)$.

Theorem 2.2. If $\psi(W, t, \tau)$ satisfies the Lipschitz condition in W, then numerical method which given by Eq (2.6) is stable.

Proof. We refer the reader to [42–44] for the details of the proof. □

Lemma 2.3. If $\|e_{n+1}\| \le (1 + \tau L_1)\|e_n\| + C$, then

$$\|e_n\| \le (1 + \tau L_1)^n \|e_0\| + \frac{C(1 + \tau L_1)^n}{\tau L} \le \frac{C}{\tau L_1} + e^{L_1 T}\|e_0\| - (e^{L_1 T} - 1). \tag{2.7}$$

where $e_n = W_n - W(t_n)$ and C is constant.

Proof. For the details of the proof, one may refer to [42–44]. □

Equation (2.6) is fourth order one-step method and the error estimate is as follows

$$|e_n| \leq e^{L_1 T}(|e_0| + L_1 \tau e + cT\tau^4), \tag{2.8}$$

where L_1 is lipschitz constant and $e = max(|e_0|, |e_1|, \cdots, |e_{n-1}|)$. Noting that $\phi_0 = \phi(t_0)$, we can obtain the global truncation error is $\boldsymbol{O}(\tau^4)$.

3. Simulation results

In this part, we use the present method to numerically solve the 3D coupled Gray-Scott models, the numerical simulation results are shown in Figures 1–9. All computations of simulation results are performed by the MatlabR2017b software.

Experiment 1. We experiment (1.1) with the diffusion coefficients in space is given as $K_u = 4 \times 10^{-5}$, $K_v = 1 \times 10^{-5}$, $F = 0.015$, $k = 0.045$, $N = 128$, $\tau = 0.01$. Initially, the entire system was placed in the trivial state $(u, v) = (1, 0)$, and a $32 \times 32 \times 32$ cube point area located symmetrically about the centre of the cube was perturbed to $(u, v) = (\frac{1}{2}, \frac{1}{4})$ and the domain is $[-1, 1]^3$. The numerical simulation results are shown in Figures 1–6.

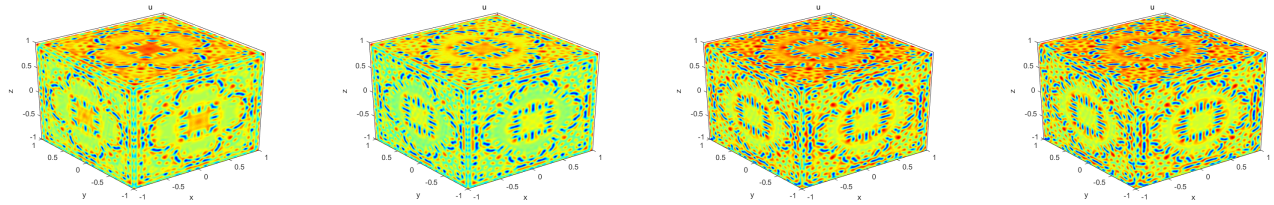

(a)$t = 5000$. (b)$t = 10000$. (c)$t = 15000$. (d)$t = 20000$.

Figure 1. The patterns of u at $\alpha = \beta = 1.8$ and different time t for Experiment 1.

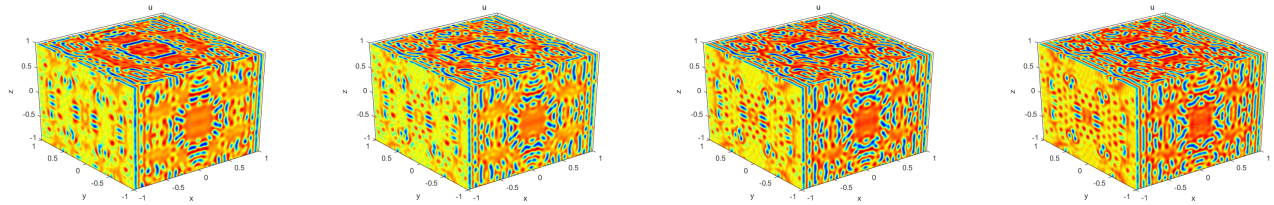

(a)$t = 5000$. (b)$t = 10000$. (c)$t = 15000$. (d)$t = 20000$.

Figure 2. The patterns of u at $\alpha = 1.8$, $\beta = 1.9$ and different time t for Experiment 1.

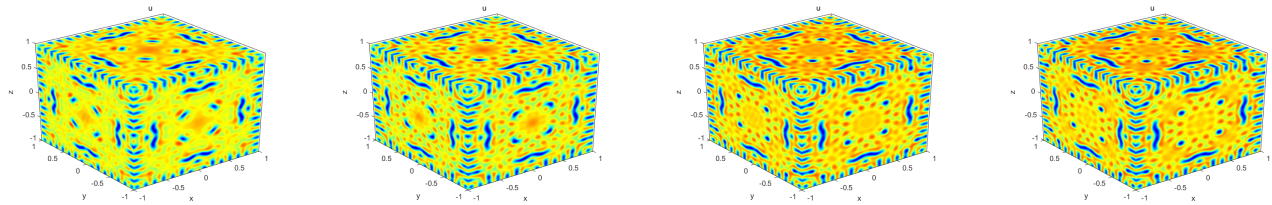

(a)$t = 5000$. (b)$t = 10000$. (c)$t = 15000$. (d)$t = 20000$.

Figure 3. The patterns of u at $\alpha = \beta = 2$ and different time t for Experiment 1.

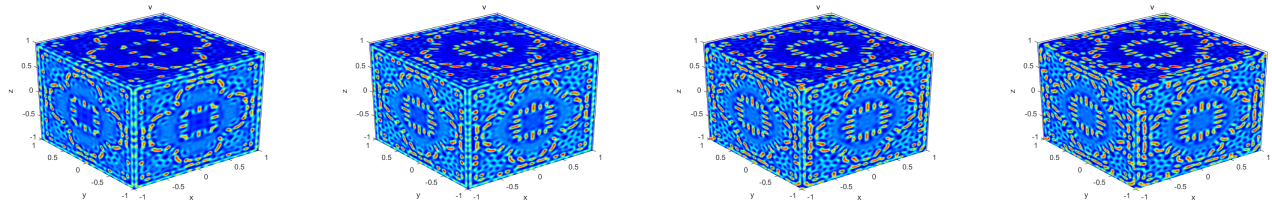

(a)$t = 5000$. (b)$t = 10000$. (c)$t = 15000$. (d)$t = 20000$.

Figure 4. The patterns of v at $\alpha = \beta = 1.8$ and different time t for Experiment 1.

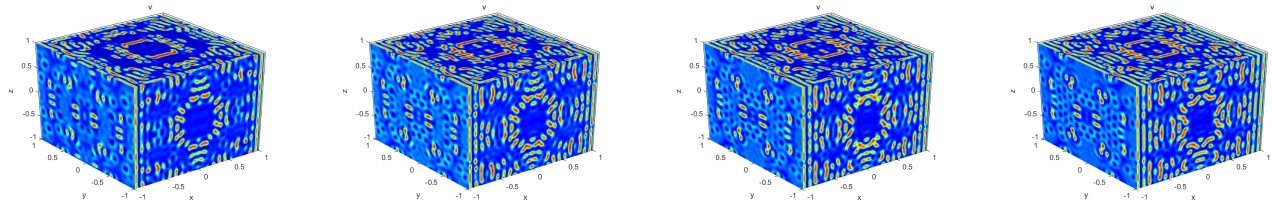

(a)$t = 5000$. (b)$t = 10000$. (c)$t = 15000$. (d)$t = 20000$.

Figure 5. The patterns of v at $\alpha = 1.8, \beta = 1.9$ and different time t for Experiment 1.

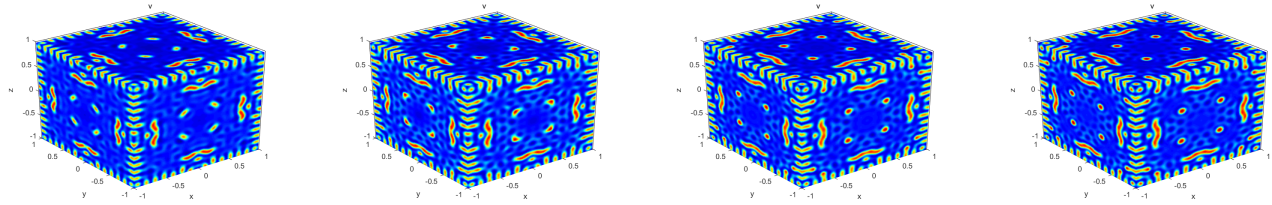

(a)$t = 5000$. (b)$t = 10000$. (c)$t = 15000$. (d)$t = 20000$.

Figure 6. The patterns of v at $\alpha = \beta = 2$ and different time t for Experiment 1.

Experiment 2. We experiment (1.1) with the diffusion coefficients in space is given as $K_u = 3 \times 10^{-5}$, $K_v = 1 \times 10^{-5}$, $F = 0.015$, $k = 0.045$, $N = 128$, $\tau = 0.01$, and on the domain size $[-1, 1] \times [-1, 1] \times [-1, 1]$. When the initial conditions is the entire system was placed in the trivial state $(u, v) = (1, 0)$, and a $32 \times 32 \times 32$ cube point area located symmetrically about the centre of the cube was perturbed to $(u, v) = (\frac{1}{2}, \frac{1}{4})$, the patterns in Figure 7 are obtained at different time t and different fractional derivative α. We experiment (1.1) with the diffusion coefficients in space is given as $K_u = 4 \times 10^{-5}$, $K_v = 1 \times 10^{-5}$, $F = 0.015$, $k = 0.045$, $N = 128$, $\tau = 0.01$, and on the domain size $[-1, 1] \times [-1, 1] \times [-1, 1]$. When

the initial conditions is the entire system was placed in the trivial state $(u, v) = (1, 0)$, the patterns in Figures 8 and 9 are obtained at different time t and different fractional derivative α. At different values of the fractional order α, we observe some the different patterns.

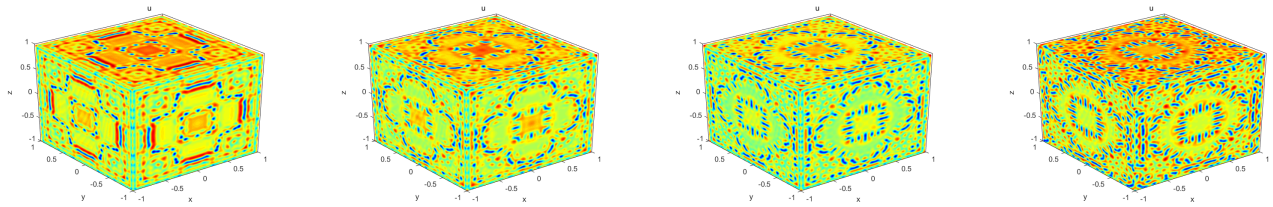

(a)$t = 1000$. (b)$t = 5000$. (c)$t = 10000$. (d)$t = 20000$.

Figure 7. The patterns of u at $\alpha = \beta = 1.8$ and different time t for Experiment 2.

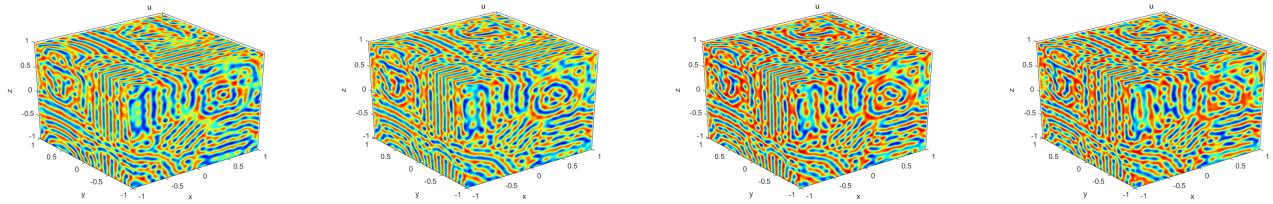

(a)$t = 4000$. (b)$t = 10000$. (c)$t = 14000$. (d)$t = 20000$.

Figure 8. The patterns of u at $\alpha = \beta = 2$ and different time t for Experiment 2.

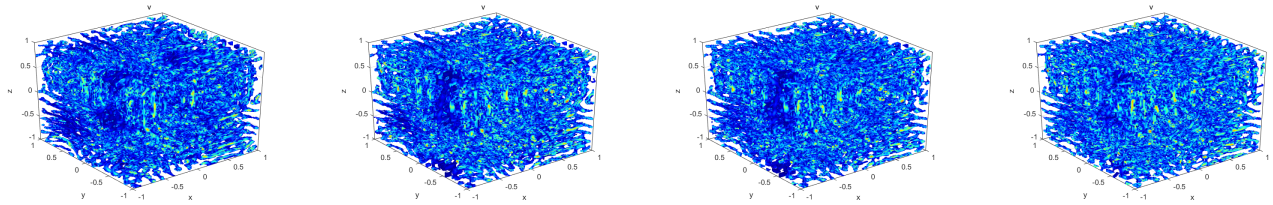

(a)$t = 4000$. (b)$t = 10000$. (c)$t = 14000$. (d)$t = 20000$.

Figure 9. The patterns of v at $\alpha = \beta = 2$ and different time t for Experiment 2.

4. Conclusions

In this paper, Fourier spectral method is used to solve the space fractional (3+1)-dimensional coupled Gray-Scott models. It is found that the results of numerical experiments are consistent with those of other scholars, which verifies the accuracy of the method. We show some patterns of space fractional 3D coupled Gray-Scott models are different from any previously obtained in numerical or theoretical studies. the influence of fractional order and long time diffusion behavior and of the space fractional (3+1)-dimensional coupled Gray-Scott models is observed. Numerical results show that this method has strong competitiveness, reliability and solving ability for solving 3D FRDM. Fourier spectral method can also be used to study other (n+1)-dimensional space variable FRDM.

Acknowledgments

The work is supported by the Natural Science Foundation of Inner Mongolia [2021MS01009].

Conflict of interest

The authors declare that there are no conflicts of interest regarding the publication of this article.

References

1. M. Abbaszadeh, M. Dehghan, A reduced order finite difference method for solving space-fractional reaction-diffusion systems: The Gray-Scott model, *Eur. Phy. J. Plus*, 2019. https://doi.org/10.1140/epjp/i2019-12951-0
2. X. L. Zhang, W. Zhang, Y. L. Wang, T. T. Ban, The space spectral interpolation collocation method for reaction-diffusion systems, *Therm. Sci.,* **25** (2021), 1269–1275. https://doi.org/10.2298/TSCI200402022Z
3. A. Mmm, B. Jar, C. Kpab, Dynamical behavior of reaction diffusion neural networks and their synchronization arising in modeling epileptic seizure: A numerical simulation study, *Comput. Math. Appl.*, **80** (2020), 1887–1927. https://doi.org/10.1016/j.camwa.2020.08.020
4. A. Atangana, R. T. Alqahtani, New numerical method and application to Keller-Segel model with fractional order derivative, *Chaos Soliton. Fract.*, **116** (2018), 14–21. https://doi.org/10.1016/j.chaos.2018.09.013
5. X. J. Yang, *General fractional derivatives: Theory, methods and applications*, New York: CRC Press, 2019. https://doi.org/10.1201/9780429284083
6. Y. L. Wang, M. J. Du, F. G. Tan, Using reproducing kernel for solving a class of fractional partial differential equation with non-classical conditions, *Appl. Math. Comput.*, **219** (2013), 5918–5925. https://doi.org/10.1016/j.amc.2012.12.009
7. N. Anjum, C. H. He, J. H. He, Two-scale fractal theory for the population dynamics, *Fractals*, **29** (2021), 2150182. https://doi.org/10.1142/S0218348X21501826
8. W. Zhang, Y. L. Wang, M. C. Wang, The reproducing kernel for the reaction-diffusion model with a time variable fractional order, *Therm. Sci.*, **24** (2020), 2553–2559. https://doi.org/10.2298/TSCI2004553Z
9. I. Podlubny, *Fractional differential equations: An introduction to fractional derivatives, fractional differential equations to methods of their solution and some of their applications*, Academic Press, 1998.
10. J. H. He, W. F. Hou, C. H. He, T. Saeed, T. Hayat, Variational approach to fractal solitary waves, *Fractals*, **29** (2021), 2150199. https://doi.org/10.1142/S0218348X21501991
11. D. Tian, Q. T. Ain, N. Anjum, C. H. He, B. Cheng, Fractal N/MEMS: From the pull-in instability to pull-in stability, *Fractals*, **29** (2020), 2150030. https://doi.org/10.1142/S0218348X21500304
12. D. Tian, C. H. He, A fractal micro-electromechanical system and its pull-in stability, *J. Low Freq. Noise V. A.*, **40** (2021), 1380–1386. https://doi.org/10.1177/1461348420984041

13. C. H. He, K. A. Gepreel, Low frequency property of a fractal vibration model for a concrete beam, *Fractals*, **29** (2021), 2150117. https://doi.org/10.1142/S0218348X21501176
14. D. Baleanu, X. J. Yang, H. M. Srivastava, Local fractional similarity solution for the diffusion equation defined on Cantor sets, *Appl. Math. Lett.*, **47** (2015), 54–60. https://doi.org/10.1016/j.aml.2015.02.024
15. A. A. Kilbas, H. M. Srivastava, J. J. Trujillo, *Theory and applications of fractional differential equations*, Elsevier, Netherlands, 2006. https://doi.org/10.1016/S0304-0208(06)80001-0
16. T. M. Atanackovic, S. Pilipovic, B. Stankovic, D. Zorica, T. M. Atanackovic, Fractional calculus with applications in mechanics: Vibrations and diffusion processes, *Drug Dev. Ind. Pharm.*, 2014. https://doi.org/10.1002/9781118577530
17. P. I. Butzer, U. Westphal, *An introduction to fractional calculus, in applications of fractional calculus in physics*, World Scientific, Singapore, 2000, 1–85. https://doi.org/10.1142/9789812817747-0001
18. S. Samko, A. Kilbas, O. Marichev, *Fractional integrals and derivatives: Theory and applications*, Gordon and Breach, Amsterdam, 1993.
19. V. V. Uchaikin, *Fractional derivatives for physicists and engineers*, Higher Education Press and Springer Verlag, Beijing/Berlin, 2013.
20. E. E. Sel'Kov, Self-oscillations in glycolysis, *Fed. Eur. Biochem. Soc. J.*, **4** (1968), 79–86.
21. P. Gray, S. K. Scott, Autocatalytic reactions in the isothermal, continuous stirred tank reactor: Isolas and other forms of multistability, *Chem. Eng. Sci.*, **38** (1983), 29–43.
22. Y. Liu, E. Y. Fan, B. L. Yin, H. Li, J. F. Wang, TT-M finite element algorithm for a two-dimensional space fractional Gray-Scott model, *Comput. Math. Appl.*, **80** (2020), 1793–1809. https://doi.org/10.1016/j.camwa.2020.08.011
23. A. Bueno-Orovio, D. Kay, K. Burrage, Fourier spectral methods for fractional-in-space reaction-diffusion equations, *BIT*, **54** (2014), 937–954. https://doi.org/10.1007/s10543-014-0484-2
24. G. H. Lee, A second-order operator splitting Fourier spectral method for fractional-in-space reaction-diffusion equations, *J. Comput. Appl. Math.*, **33** (2018), 395–403. https://doi.org/10.1016/j.cam.2017.09.007
25. T. T. Wang, F. Y. Song, H. Wang, G. E. Karniadakis, Fractional gray-scott model: Well-posedness, discretization, and simulations, *Comput. Method. Appl. M.*, **347** (2019), 1030–1049. https://doi.org/10.1016/j.cma.2019.01.002
26. M. Abbaszadeh, M. Dehghan, I. M. Navon, A pod reduced-order model based on spectral Galerkin method for solving the space-fractional Gray-Scott model with error estimate, *Eng. Comput.*, 2020, 1–24. https://doi.org/10.1007/s00366-020-01195-5
27. K. M. Owolabi, B. Karaagac, Dynamics of multi-pulse splitting process in one-dimensional Gray-Scott system with fractional order operator, *Chaos Soliton. Fract.*, **136** (2020). https://doi.org/10.1016/j.chaos.2020.109835
28. W. Wang, Y. Lin, Y. Feng, L. Zhang, Y. J. Tan, Numerical study of pattern formation in an extended Gray-Scott model, *Commun. Nonlinear Sci.*, **16** (2011), 2016–2026. https://doi.org/10.1016/j.cnsns.2010.09.002

29. T. Chen, S. M. Li, J. Llibr, Phase portraits and bifurcation diagram of the Gray-Scott model-sciencedirect, *J. Math. Anal. Appl.*, **496** (2020), 124840. https://doi.org/10.1016/j.jmaa.2020.124840

30. V. Daftardar-Gejji, Y. Sukale, S. Bhalekar, A new predictor-corrector method for fractional differential equations, *Appl. Math. Comput.*, **244** (2014), 158–182. https://doi.org/10.1016/j.amc.2014.06.097

31. A. Jhinga, V. Daftardar-Gejji, A new finite difference predictor-corrector method for fractional differential equations, *Appl. Math. Comput.*, **336** (2018), 418–432. https://doi.org/10.1016/j.amc.2018.05.003

32. Y. Zhang, J. Cao, W. Bu, A. Xiao, A fast finite difference/finite element method for the two-dimensional distributed-order time-space fractional reaction-diffusion equation, *Int. J. Model. Simul. SC*, **11** (2020), 2050016. https://doi.org/10.1142/S1793962320500166

33. Y. L. Wang, L. N. Jia, H. L. Zhang, Numerical solution for a class of space-time fractional equation in reproducing, *Int. J. Comput. Math.*, **96** (2019), 2100–2111. https://doi.org/10.1080/00207160.2018.1544367

34. F. Z. Geng, X. Y. Wu, Reproducing kernel function-based Filon and Levin methods for solving highly oscillatory integral, *Appl. Math. Comput.*, **397** (2021), 125980. https://doi.org/10.1016/j.amc.2021.125980

35. X. Y. Li, B. Y. Wu, A new reproducing kernel method for variable order fractional boundary value problems for functional differential equations, *J. Comput. Appl. Math.*, **311** (2017), 387–393. https://doi.org/10.1016/j.cam.2016.08.010

36. X. Y. Li, B. Y. Wu, Error estimation for the reproducing kernel method to solve linear boundary value problems, *J. Comput. Appl. Math.*, **243** (2013), 10–15. https://doi.org/10.1016/j.cam.2012.11.002

37. F. Z. Geng, X. Y. Wu, Reproducing kernel functions based univariate spline interpolation, *Appl. Math. Lett.*, **122** (2021), 107525. https://doi.org/10.1016/j.aml.2021.107525

38. X. Y. Li, B. Y. Wu, Superconvergent kernel functions approaches for the second kind Fredholm integral equations, *Appl. Numer. Math.*, **67** (2021), 202–210. https://doi.org/10.1016/j.apnum.2021.05.004

39. X. Y. Li, H. L. Wang, B. Y. Wu, An accurate numerical technique for fractional oscillation equations with oscillatory solutions, *Math. Method. Appl. Sci.*, **45** (2022), 956–966. https://doi.org/10.1002/mma.7825

40. D. D. Dai, T. T. Ban, Y. L. Wang, W. Zhao, The piecewise reproducing kernel method for the time variable fractional order advection-reaction-diffusion equations, *Therm. Sci.*, **25** (2021), 1261–1268. https://doi.org/10.2298/TSCI200302021D

41. I. Podlubny, Matrix approach to discrete fractional calculus, *Fract. Calc. Appl. Anal.*, **3** (2000), 359–386. https://doi.org/10.1016/j.jcp.2009.01.014

42. C. Han, Y. L. Wang, Z. Y. Li, A high-precision numerical approach to solving space fractional Gray-Scott model, *Appl. Math. Lett.*, **125** (2022), 107759. https://doi.org/10.1016/j.aml.2021.107759

43. C. Han, Y. L. Wang, Z. Y. Li, Numerical solutions of space fractional variable-coefficient KdV-modified KdV equation by Fourier spectral method, *Fractals*, **29** (2021), 2150246. https://doi.org/10.1142/S0218348X21502467

44. X. Y. Li, C. Han, Y. L. Wang, Novel patterns in fractional-in-space nonlinear coupled fitzhugh-nagumo models with Riesz fractional derivative, *Fractal Fract.*, **6** (2022), 136. https://doi.org/10.3390/fractalfract6030136

45. J. S. Duan, D. C. Hu, M. Li, Comparison of two different analytical forms of response for fractional oscillation equation, *Fractal Fract.*, **5** (2021), 188. https://doi.org/10.3390/fractalfract5040188

46. Q. T. Ain, J. H. He, N. Anjum, M. Ali, The fractional complex transform: A novel approach to the time-fractional Schrödinger equation, *Fractals*, **28** (2020), 2050141. https://doi.org/10.1142/S0218348X20501418

AIMS Press